

Increased Expression of Catalase and Superoxide Dismutase 2 Reduces Cone Cell Death in Retinitis Pigmentosa

Shinichi Usui^{1,2}, Keiichi Komeima^{1,2}, Sun Young Lee^{1,2}, Young-Joon Jo^{1,2}, Shinji Ueno^{1,2}, Brian S Rogers^{1,2}, Zhihao Wu^{1,2}, Jikui Shen^{1,2}, Lili Lu^{1,2}, Brian C Oveson^{1,2}, Peter S Rabinovitch³ and Peter A Campochiaro^{1,2}

¹Department of Ophthalmology, Johns Hopkins University School of Medicine, Baltimore, Maryland, USA; ²Department of Neuroscience, Johns Hopkins University School of Medicine, Baltimore, Maryland, USA; ³Department of Pathology, University of Washington, Seattle, Washington, USA

Oxidative and nitrosative damage are major contributors to cone cell death in retinitis pigmentosa (RP). In this study, we explored the effects of augmenting components of the endogenous antioxidant defense system in models of RP, *rd1*, and *rd10* mice. Unexpectedly, overexpression of superoxide dismutase 1 (SOD1) in *rd1* mice increased oxidative damage and accelerated cone cell death. With an elaborate mating scheme, genetically engineered *rd10* mice with either inducible expression of SOD2, Catalase, or both in photoreceptor mitochondria were generated. Littermates with the same genetic background that did not have increased expression of SOD2 nor Catalase provided ideal controls. Coexpression of SOD2 and Catalase, but not either alone, significantly reduced oxidative damage in the retinas of postnatal day (P) 50 *rd10* mice as measured by protein carbonyl content. Cone density was significantly greater in P50 *rd10* mice with coexpression of SOD2 and Catalase together than *rd10* mice that expressed SOD2 or Catalase alone, or expressed neither. Coexpression of SOD2 and Catalase in *rd10* mice did not slow rod cell death. These data support the concept of bolstering the endogenous antioxidant defense system as a gene-based treatment strategy for RP, and also indicate that coexpression of multiple components may be needed.

Received 6 January 2009; accepted 11 February 2009; published online 17 March 2009. doi:10.1038/mt.2009.47

INTRODUCTION

Retinitis pigmentosa (RP) is a group of diseases in which one of several different mutations results in death of rod photoreceptor cells. The loss of rods results in night blindness, but patients are still able to function well if illumination is adequate. However, once rods die, there is gradual loss of cones accompanied by constriction of visual fields and eventual blindness. If cone death could be prevented in patients with RP, blindness could be averted.

The outer portion of the retina consists solely of photoreceptors, and rods vastly outnumber cones. After rods die, oxygen

utilization in the outer retina is reduced, but because choroidal vessels, unlike retinal vessels, are incapable of autoregulation to decrease blood flow when tissue oxygen levels are increased, the oxygen level in the outer retina becomes markedly elevated.^{1,2} After rods are eliminated, there is progressive oxidative and nitrosative damage to cones, which are major contributors to their death.^{3,4} In several models of RP in which rods die from different mutations, exogenous antioxidants slow cone cell death, indicating a potential therapeutic approach in all RP patients despite tremendous heterogeneity in pathogenic mutations.⁵

When free radicals are generated they interact with the first available acceptor they contact, and for antioxidants to prevent damage to critical molecules, they must be present in sufficiently high concentrations in correct cellular compartments to reduce chance meetings of radicals with those molecules. This is a difficult requirement for exogenous antioxidants that must penetrate into all cellular compartments and maintain high levels at all times. Bolstering the endogenous antioxidant defense system may provide a more efficient approach that could be used in a complementary fashion. In this study, we sought to explore the effects of increasing levels of components of the antioxidant defense system in photoreceptors on cone survival in models of RP.

RESULTS

Paradoxical effect of overexpression of SOD1 in *rd1*^{+/+} mice

In order to determine if increased levels of superoxide dismutase 1 (SOD1) could slow or prevent cone cell death in a primary rod cell degeneration, transgenic mice in which the *actin* promoter drives expression of human SOD1 were crossed with *rd1*^{+/+} mice and offspring were crossed to obtain *rd1*^{+/+} mice that carry the *Sod1* transgene (*Sod1-rd1*^{+/+} mice). At postnatal day (P) 25, there was strong expression of human SOD1 in *Sod1-rd1*^{+/+} mice and no detectable expression in *rd1*^{+/+} mice (Figure 1a), but surprisingly *Sod1-rd1*^{+/+} mice showed significantly greater carbonyl adducts on proteins in the retina than did *rd1*^{+/+} mice, indicating increased rather than decreased oxidative damage (Figure 1b). At P35, compared to *rd1*^{+/+} mice, *Sod1-rd1*^{+/+} mice showed reduced cone density in all four quadrants of the retina (Figure 1c,d). There was also a reduction

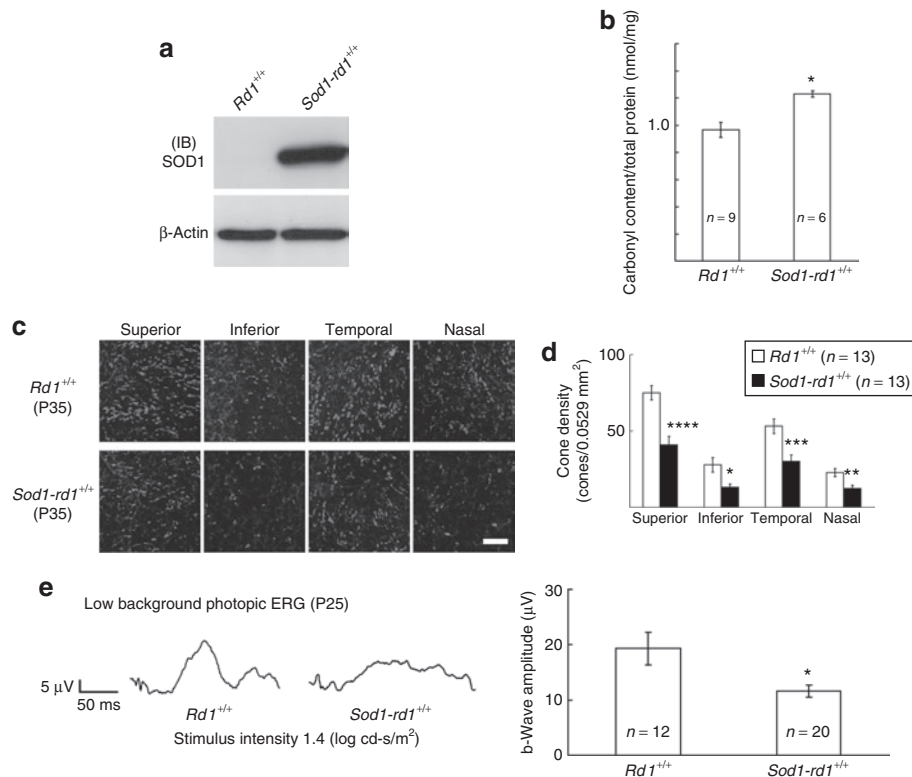


Figure 1 Superoxide dismutase 1 (SOD1) overexpression significantly decreases cone function and cone cell number in *rd1*^{+/+} mice. Transgenic mice in which the *actin* promoter drives expression of human SOD1 were crossed with *rd1*^{+/+} mice and offspring were crossed to obtain *rd1*^{+/+} mice that carried the *Sod1* transgene (*Sod1-rd1*^{+/+} mice). **(a)** At postnatal day (P) 25, *rd1*^{+/+} and *Sod1-rd1*^{+/+} mice were euthanized and retinal homogenates were run in western blots using an antibody directed against human SOD1. Immunoblots (IBs) showed strong expression of human SOD1 in *Sod1-rd1*^{+/+} and no detectable expression in *rd1*^{+/+} mice. Stripping and reprobing of IBs with an antibody directed against β-actin showed that loading was equivalent. **(b)** At P25, the mean (±SEM) number of carbonyl adducts determined by enzyme-linked immunosorbent assay of retinal homogenates showed a significant increase in oxidized proteins in *Sod1-rd1*^{+/+} mice (*n* = 6) compared to *rd1* mice (*n* = 9; **P* < 5.0 × 10⁻⁴ by unpaired Student's *t*-test). **(c)** At P35, compared to *rd1* mice, *Sod1-rd1*^{+/+} mice appeared to show lower cone density in all four quadrants of the retina by confocal microscopy of peanut agglutinin-stained retinal flat mounts (scale bar = 50 μm) and this was confirmed by image analysis **(d)**; **P* < 2.0 × 10⁻⁴, ***P* < 0.02, ****P* < 0.002, *****P* < 0.01 by unpaired Student's *t*-test). **(e)** Representative wave forms from photopic electroretinograms (ERGs) done in low background illumination at P25 showed lower b-waves for *Sod1-rd1*^{+/+} mice than *rd1*^{+/+} mice and measurements confirmed a significant reduction in mean (±SEM) b-wave amplitude *Sod1-rd1*^{+/+} mice (**P* < 0.05 by unpaired Welch's *t*-test).

in mean photopic b-wave amplitude in P35 *Sod1-rd1*^{+/+} mice compared to *rd1*^{+/+} mice, indicating that loss of cone cell function was accelerated by overexpression of SOD1 in *rd1*^{+/+} mice.

Generation of transgenic mice with inducible expression of SOD2, Catalase, or both

We have previously used the tet/on inducible system to test the effects of overexpressing many different proteins in photoreceptors.⁶⁻¹⁰ To explore the effects of overexpressing components of the antioxidant defense system, we generated *tetracycline response element (TRE)/Sod2* mice and *TRE/Catalase* mice. The peroxisomal targeting signal was deleted from the *Catalase* transgene and an ornithine transcarbamylase signal sequence was added to direct the Catalase to mitochondria (Figure 2a). The reverse tetracycline transactivator/interphotoreceptor retinol-binding protein promoter (*rtTA/IRBP*) was used as the driver line, because it directs expression in both rods and cones. *Rd10*^{+/+} mice were used for these experiments, because retinal degeneration occurs more slowly in *rd10*^{+/+} mice than *rd1*^{+/+} mice. Mice homozygous at both the *rtTA/IRBP* and *rd10* alleles were generated and crossed with mice homozygous at the *rd10* allele, but heterozygous at the *TRE/Sod2*

and *TRE/Catalase* alleles and the possible offspring are shown in Figure 2b. The offsprings were genotyped and after weaning they were given normal drinking water or drinking water containing 2 mg/ml of doxycycline, and then mitochondrial fractions of retinal homogenates were run in immunoblots. A fairly consistent baseline level of murine SOD2 was seen in all samples except those from doxycycline-treated mice that carried the *TRE/Sod2* transgene (Figure 2c). Likewise, strong bands for human Catalase were seen only in samples from doxycycline-treated mice that carried the *TRE/Catalase* transgene. All samples showed similar bands for COX4, which is expressed in mitochondria, indicating that roughly equivalent amounts of mitochondrial fractions had been loaded. These data demonstrate that mice with either inducible expression of SOD2, Catalase, or both in the mitochondria of photoreceptors had been generated.

Rd10^{+/+} mice with induced expression of SOD2 and Catalase in photoreceptors show reduced superoxide radicals in the retina

Hydroethidine is taken up into cells and in the presence of superoxide radicals is converted to ethidium, which binds DNA and emits

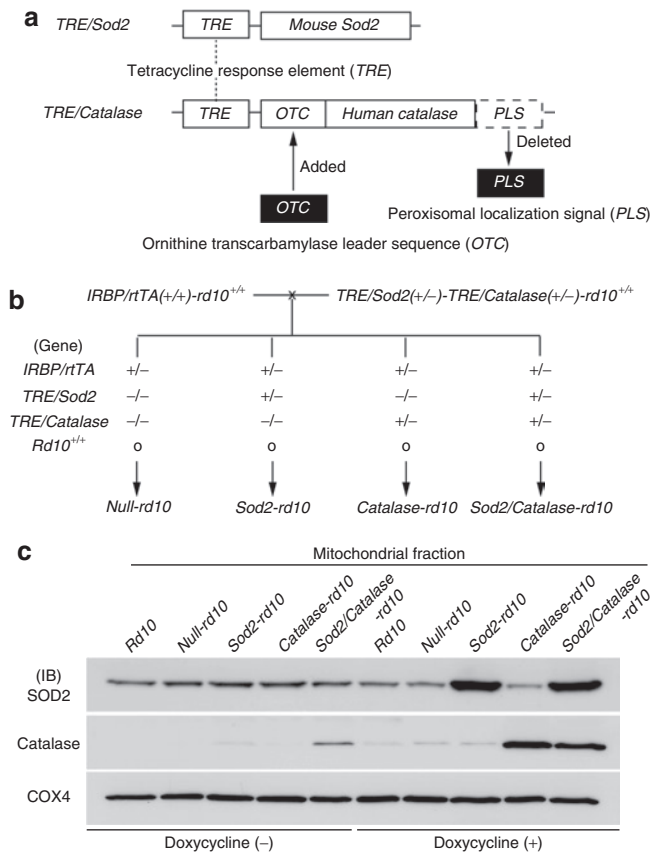


Figure 2 *Rd10^{+/+}* mice with inducible increased expression of superoxide dismutase 2 (SOD2) and Catalase in the mitochondria of photoreceptors. **(a)** Schematic diagram of the *TRE/Sod2* and *TRE/Catalase* transgenes are shown. The tetracycline response element (TRE) was coupled to the full-length cDNA for mouse *Sod2*. The ornithine transcarbamylase (OTC) leader sequence, which mediates mitochondrial localization, was ligated to the N terminus cDNA for human *Catalase* and the peroxisomal localization signal (PLS) was deleted from the C terminus prior to coupling to the TRE. Using these constructs, *TRE/Sod2* and *TRE/Catalase* transgenic mice were generated. **(b)** Multiple crosses were done to generate *TRE/Sod2(+/-)-TRE/Catalase(+/-)-rd10^{+/+}* mice and homozygous *interphotoreceptor retinol-binding protein promoter/reverse tetracycline transactivator-rd10^{+/+}* mice (*IRBP/rtTA(+/+)-rd10^{+/+}* mice). These two types of mice were crossed to yield four groups of offspring, *null-rd10^{+/+}*, *Sod2-rd10^{+/+}*, *Catalase-rd10^{+/+}*, and *Sod2/Catalase-rd10^{+/+}* mice for which the genotypes are shown. **(c)** *Null-rd10^{+/+}*, *Sod2-rd10^{+/+}*, *Catalase-rd10^{+/+}*, and *Sod2/Catalase-rd10^{+/+}* mice were given normal drinking water or water supplemented with 2mg/ml of doxycycline between postnatal day (P) 10 and P25. Mice were euthanized and the mitochondrial fractions of retinal homogenates were run in immunoblots using antibodies specific for murine SOD2, human Catalase, and murine cyclooxygenase 4 (COX4), which is known to localize to mitochondria. Background levels of murine SOD2 were seen in retinal mitochondria of all mice, but when treated with doxycycline, only *Sod2-rd10^{+/+}* and *Sod2/Catalase-rd10^{+/+}* mice showed a substantial increase in SOD2. Likewise, when treated with doxycycline *Catalase-rd10^{+/+}* and *Sod2/Catalase-rd10^{+/+}* showed strong bands for Catalase. Strong bands for COX4 were seen in the retinal mitochondria of all mice.

red fluorescence providing a means to visualize production of superoxide radicals *in situ*.¹¹ We previously utilized this technique to show that there is a striking increase in superoxide radicals in the outer retinas of P30 *rd1^{+/+}* mice in which rods have degenerated.¹² At P35, wild-type mice showed minimal fluorescence in

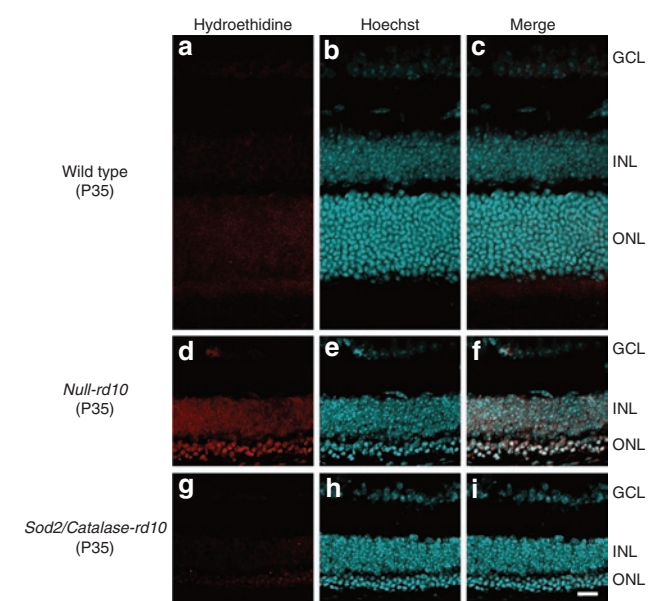


Figure 3 Coexpression of superoxide dismutase 2 (SOD2) and Catalase in mitochondria reduce superoxide radicals in the retinas of *rd10^{+/+}* mice. At postnatal day (P) 35, hydroethidine was injected intraperitoneally into wild-type mice ($n = 4$), *null-rd10^{+/+}* mice treated with doxycycline between P10 and P35 as described in Materials and Methods ($n = 4$), or *Sod2/Catalase-rd10^{+/+}* mice treated with doxycycline between P10 and P35 ($n = 4$) and after 18 hours the mice were euthanized and ocular sections were examined by confocal microscopy. Representative sections showed minimal fluorescence in the retinas of wild-type mice (**a-c**), strong fluorescence primarily in the remaining outer nuclear layer (ONL) and outer plexiform layer of the retinas of *null-rd10^{+/+}* mice (**d-f**), and minimal fluorescence in the retinas of *Sod2/Catalase-rd10^{+/+}* mice (**g-i**). This demonstrates a marked increase in superoxide radicals in the outer retina of mice after degeneration of rods that is reduced by coexpression of SOD2 and Catalase. Scale bar = 20 μ m. GCL, ganglion cell layer; INL, inner nuclear layer.

the retina when hydroethidine had been injected prior to death (**Figure 3a**) indicating low levels of superoxide radicals, but P35 *rd10^{+/+}* mice showed strong fluorescence in the outer retina indicating high levels of superoxide radicals (**Figure 3b**). In contrast, P35 *rd10^{+/+}* mice with coexpression of SOD2 and Catalase in the mitochondria of photoreceptors showed little fluorescence in the retina when hydroethidine had been injected prior to death (**Figure 3c**), indicating a large increase in the capacity to scavenge superoxide radicals.

Increased expression of Catalase and SOD2 significantly reduce carbonyl content in the retinas of *rd10^{+/+}* mice

When proteins undergo oxidative damage, the most common modification is introduction of carbonyl groups into side chains,¹³ and enzyme-linked immunosorbent assay (ELISA) for carbonyl adducts provides a quantitative measure of oxidative damage.^{14,15} To determine if the increased capacity to neutralize superoxide radicals translated into protection from oxidative damage we measured carbonyl levels in the retina by ELISA. At P35, a time point when rod degeneration is just being completed in *rd10^{+/+}* mice, there was no difference in carbonyl levels in the retinas of mice with increased expression of Catalase or both Catalase and SOD2

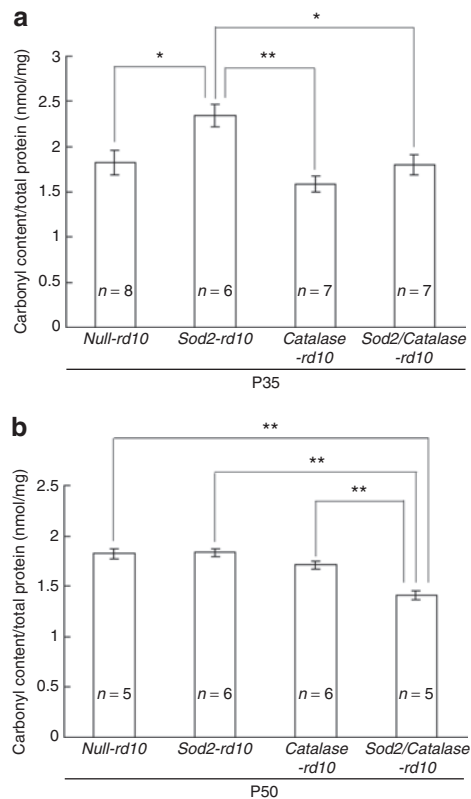


Figure 4 Increased expression of Catalase and superoxide dismutase 2 (SOD2) significantly reduce carbonyl content in the retinas of postnatal day (P) 50 *rd10*^{+/+} mice. Starting at P10, the mothers of *null-rd10*^{+/+}, *Sod2-rd10*^{+/+}, *Catalase-rd10*^{+/+}, and *Sod2/Catalase-rd10*^{+/+} mice and after weaning the mice themselves were treated with doxycycline. Mice were euthanized at P35 or P50 and protein carbonyl content was measured by enzyme-linked immunosorbent assay of retinal homogenates. At P35, the mean (±SEM) carbonyl content per mg retinal protein was significantly greater in *Sod2-rd10*^{+/+} mice than *null-rd10*^{+/+}, *Catalase-rd10*^{+/+}, or *Sod2/Catalase-rd10*^{+/+} mice (**a**; **P* < 0.05; ***P* < 0.01 by Tukey–Kramer test). At P50, the mean (±SEM) carbonyl content per mg retinal protein was significantly less in *Sod2/Catalase-rd10*^{+/+} mice compared to *null-rd10*^{+/+}, *Sod2-rd10*^{+/+}, or *Catalase-rd10*^{+/+} mice (**b**; ***P* < 0.01 by Tukey–Kramer test).

in photoreceptor mitochondria compared to *null-rd10*^{+/+} mice that did not have increased expression of an antioxidant enzyme (**Figure 4a**). However, *Sod2-rd10*^{+/+} mice had significantly greater carbonyl content per mg retinal protein than *null-rd10*^{+/+}, *Catalase-rd10*^{+/+}, or *Sod2/Catalase-rd10*^{+/+} mice, indicating that increased production of SOD2 in photoreceptors increased oxidative damage in *rd10*^{+/+} mice. At P50, when cones have been present with no surrounding rods for ~2 weeks, carbonyl content per mg retinal protein was significantly less in *Sod2/Catalase-rd10*^{+/+} mice compared to *null-rd10*^{+/+}, *Sod2-rd10*^{+/+}, or *Catalase-rd10*^{+/+} mice (**Figure 4b**). This indicates that coexpression of SOD2 and Catalase, but not expression of either of them alone reduces oxidative damage in cones after rods have degenerated.

Increased expression of SOD2 and Catalase in mitochondria of photoreceptors decreases cone cell death in *rd10*^{+/+} mice

Fluorescence confocal microscopy of peanut agglutinin–stained retinal flat mounts provides a means of assessing cone cell density

and, hence, cone survival, provided the same region of the retina is evaluated at different time points.⁴ In comparison to P18 wild-type mice, there is no difference in cone density in P18 or P35 *rd10* mice (**Figure 5a**); however, between P35 and P50, there is substantial loss of cones. This is consistent with observations in multiple models of RP, indicating that cone density is relatively stable until rod degeneration is essentially complete, and then gradual loss of cones occurs.^{4,5} However, while the number of cones is similar in P18 and P35 *rd10*^{+/+} mice, cone morphology is abnormal at P35, because outer segments are missing and inner segments are flattened, indicating that cones are under considerable stress (**Figure 5a**). When mice were treated with doxycycline starting at P18, cone density at P50 was significantly greater in *Sod2/Catalase-rd10*^{+/+} mice compared to *null-rd10*^{+/+}, *Sod2-rd10*^{+/+}, or *Catalase-rd10*^{+/+} (**Figure 5b–d**). Cone density was not greater in *Sod2-rd10*^{+/+} or *Catalase-rd10*^{+/+} compared to *null-rd10*^{+/+} mice. This indicates that coexpression of SOD2 and Catalase in the mitochondria of cones, but not either alone, promotes cone survival after rods have degenerated in *rd10*^{+/+} mice. In contrast to this robust effect on cone survival, coexpression of SOD2 and Catalase, as well as expression of either alone, had no effect on rod survival in *rd10*^{+/+} mice as demonstrated by failure to prevent thinning of the outer nuclear layer (ONL) at P25 and P35 (**Figure 6**).

Increased expression of SOD2 and Catalase preserves cone cell function in P50 *rd10*^{+/+} mice

There was no difference in mean scotopic electroretinogram (ERG) b-wave amplitude at P35 in doxycycline-treated *null-rd10*^{+/+}, *Sod2-rd10*^{+/+}, *Catalase-rd10*^{+/+}, and *Sod2/Catalase-rd10*^{+/+} mice, indicating that expression of SOD2 and/or Catalase had no effect on rod function in *rd10*^{+/+} mice (**Figure 7a**). At P50, low background photopic ERGs showed nearly flat waveforms in doxycycline-treated *null-rd10*^{+/+}, *Sod2-rd10*^{+/+}, and *Catalase-rd10*^{+/+} mice, but *Sod2/Catalase-rd10*^{+/+} mice showed a substantially better waveform and significantly greater mean photopic b-wave amplitude (**Figure 7b**). This indicates that coexpression of SOD2 and Catalase in mitochondria of photoreceptors, but not expression of either of them alone, preserves cone cell function after rods have degenerated in *rd10*^{+/+} mice.

DISCUSSION

There is mounting evidence that after rods die in RP, cones are exposed to oxidative stress and gradually die from progressive oxidative and nitrosative damage.^{3–5,12} Systemically administered antioxidants or nitric oxide synthase inhibitors slow cone cell death and provide a new treatment strategy that may be applicable to all patients with RP, despite different pathogenic mutations. However, antioxidant dietary supplements are inefficient, because it is difficult to constantly maintain sufficient levels in all cellular compartments in target tissues. This problem is magnified in the retina, because access of many agents is reduced by the blood–retinal barrier. A complementary strategy is to circumvent delivery problems by local increased production of components of the endogenous antioxidant defense system. The SODs are key defenders against assault from oxidative stress in many tissues, including the retina, where deficiency of SOD1 markedly

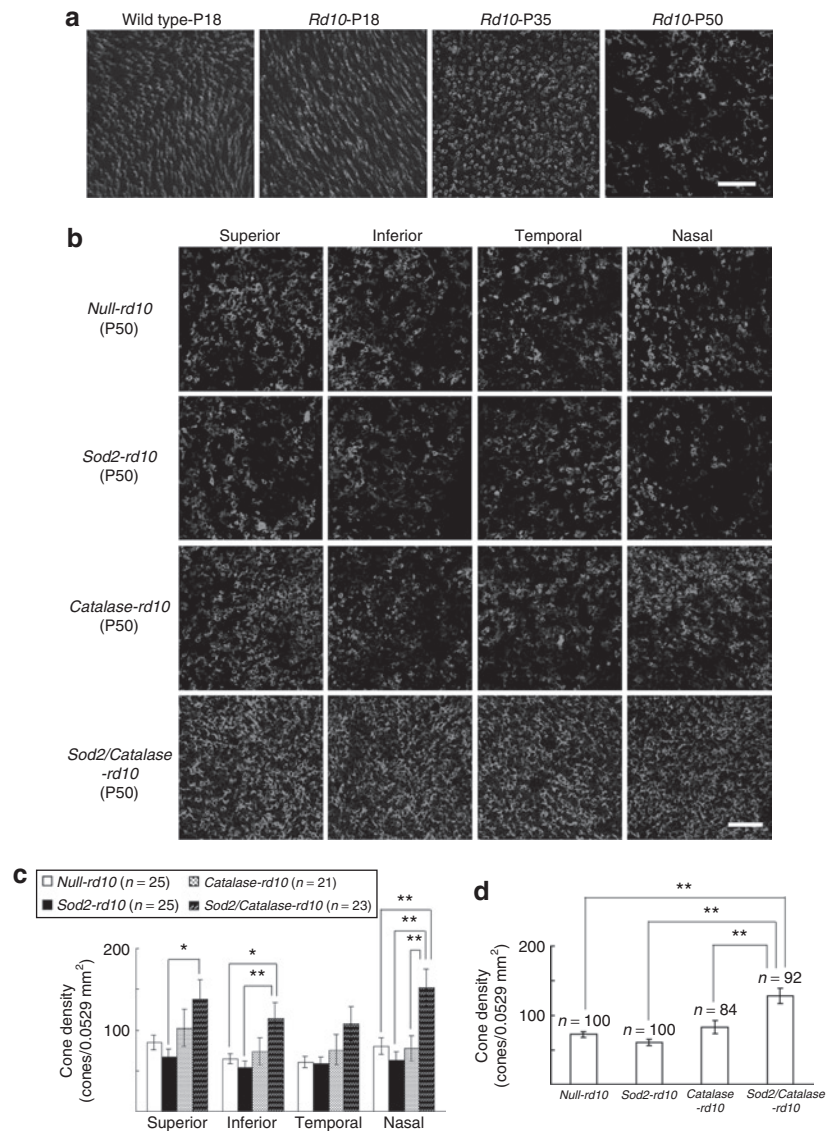


Figure 5 Increased expression of superoxide dismutase 2 (SOD2) and Catalase in mitochondria of photoreceptors decreases cone cell death in *rd10*^{+/+} mice. **(a)** Fluorescence confocal microscopy of peanut agglutinin (PNA)-stained retinal flat mounts showed little difference in cone cell density in 0.0529 mm² bins 0.5 mm superior to the center of the optic nerve in *rd10*^{+/+} mice at postnatal day (P) 18 or 35 compared to wild-type mice at P18, but by P50 there was an obvious reduction in cone density in *rd10*^{+/+} mice. At P18, outer segments were seen in wild-type and *rd10*^{+/+} mice, but at P35 and P50, *rd10*^{+/+} mice had flattened inner segments and no outer segments. Scale bar = 50 μm. **(b)** Starting at P10, the mothers of *null-rd10*^{+/+}, *Sod2-rd10*^{+/+}, *Catalase-rd10*^{+/+}, and *Sod2/Catalase-rd10*^{+/+} mice were treated with doxycycline in their drinking water. After weaning, the mice themselves were treated with doxycycline. At P50, mice were euthanized and fluorescence microscopy of PNA-stained retinal flat mounts in 0.0529 mm² bins 0.5 mm superior, inferior, temporal, and nasal to the center of the optic nerve are shown. *Sod2/Catalase-rd10*^{+/+} mice appeared to have greater cone density in all four regions of the retina compared to *null-rd10*^{+/+}, *Sod2-rd10*^{+/+}, and *Catalase-rd10*^{+/+} mice. *Sod2-rd10*^{+/+} mice appeared to have the lowest cone density. Scale bar = 50 μm. **(c)** Quantification of cone density by image analysis in each of the four 0.0529 mm² bins showed that *Sod2/Catalase-rd10*^{+/+} mice had significantly greater mean (±SEM) cone density than *Sod2-rd10*^{+/+} mice in the superior, inferior, and nasal quadrants of the retina (**P* < 0.05, ***P* < 0.01 by Tukey–Kramer test). *Sod2/Catalase-rd10*^{+/+} mice had significantly greater cone density than *null-rd10*^{+/+} mice in the inferior and nasal quadrants. *Sod2/Catalase-rd10*^{+/+} mice had significantly greater cone density than *Catalase-rd10* mice in the nasal quadrant. Scale bar = 50 μm. **(d)** Cone density measurements from each of the four quadrants in each mouse were consolidated to provide a single cone density measurement per retina. The mean (±SEM) cone density per retina was significantly greater in P50 *Sod2/Catalase-rd10*^{+/+} mice compared to *null-rd10*^{+/+}, *Sod2-rd10*^{+/+}, or *Catalase-rd10*^{+/+} mice (***P* < 0.01 by Tukey–Kramer test).

increases vulnerability to oxidative stress.¹⁶ Therefore, we first tested the concept of utilizing the endogenous antioxidant defense system in RP by exploring the effect of increased expression of SOD1 in *rd1*^{+/+} mice. Contrary to our initial expectations, rather than protecting cones in *rd1*^{+/+} mice, overexpression of SOD1 accelerated their loss of function and death (Figure 1). Similar

toxic effects were seen when SOD1 or 2 were overexpressed in cultured retinal pigmented epithelial cells.¹⁰ It appears that excess production of H₂O₂ contributes to the toxic effects of overexpression of the SODs, because coexpression of the cytosolic form of glutathione peroxidase 4 (cGpx4) with SOD1 eliminated its toxicity. Coexpression of cGpx4 with SOD2 did not eliminate its

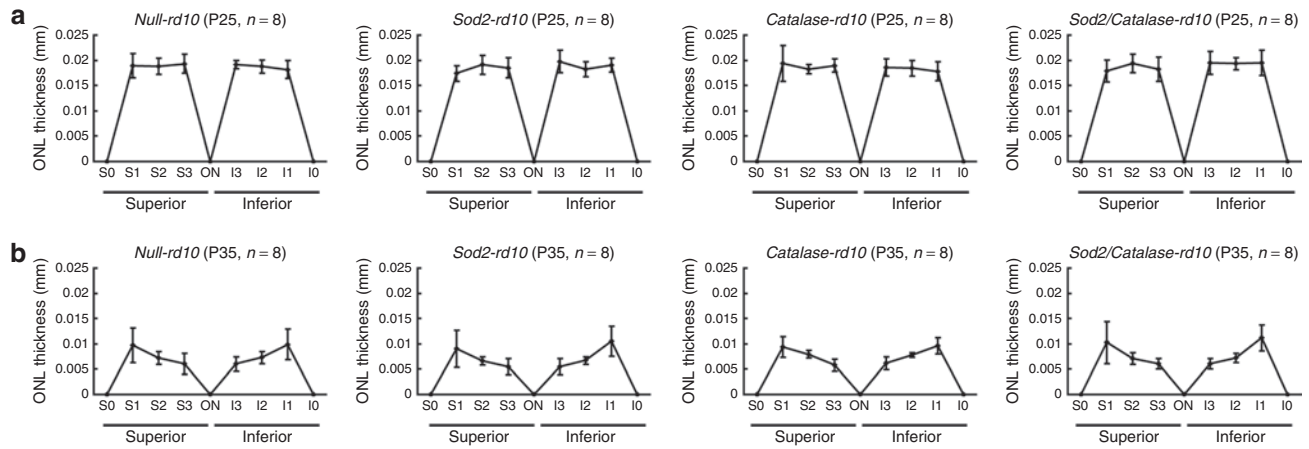


Figure 6 Overexpression of superoxide dismutase 2 (SOD2) and/or Catalase does not prevent rod cell death in *rd10*^{+/+} mice. Rod cell death leads to progressive thinning of the outer nuclear layer (ONL) in *rd10*^{+/+} mice. Measurement of ONL thickness of doxycycline-treated mice showed no significant differences by Tukey–Kramer test between *null-rd10*^{+/+}, *Sod2-rd10*^{+/+}, *Catalase-rd10*^{+/+}, and *Sod2/Catalase-rd10*^{+/+} mice at P25 (**a**) and P35 (**b**). The bars show the mean (\pm SD).

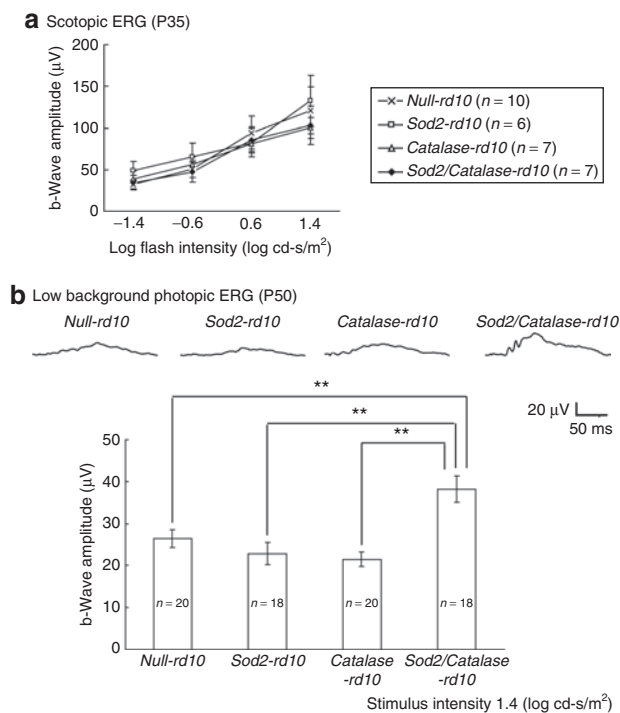


Figure 7 Increased expression of superoxide dismutase 2 (SOD2) and Catalase preserves some cone cell function at postnatal day (P) 50 in *rd10*^{+/+} mice. (**a**) Scotopic electroretinograms (ERGs) were done at P35 in *null-rd10*^{+/+}, *Sod2-rd10*^{+/+}, *Catalase-rd10*^{+/+}, and *Sod2/Catalase-rd10*^{+/+} mice treated with doxycycline. The mean (\pm SEM) b-wave amplitude for four different stimulus intensities is plotted for each of four groups of mice and there were no significant differences. (**b**) Low background photopic ERGs were done as described in Materials and Methods at P50. Representative waveforms are shown for each of the four groups and illustrate a substantially better waveform in *Sod2/Catalase-rd10*^{+/+} mice compared to *null-rd10*^{+/+}, *Sod2-rd10*^{+/+}, or *Catalase-rd10*^{+/+} mice. The bars show mean (\pm SEM) photopic b-wave amplitude, which was significantly higher (** $P < 0.01$ by Tukey–Kramer test) for *Sod2/Catalase-rd10*^{+/+} mice compared to the other three types of mice.

toxicity, suggesting that it may be necessary to express a peroxide-metabolizing enzyme in the same cellular compartment as an overexpressed SOD to maximize benefit and minimize risk. Since oxidative stress is particularly severe in mitochondria in hyperoxic tissues and photoreceptors are packed with mitochondria, we decided to target this cellular compartment. In this study, we have demonstrated that increased expression of SOD2 and Catalase in the mitochondria of photoreceptors of *rd10*^{+/+} mice reduced superoxide radicals and oxidative damage in the retina, provided significant preservation of cone function, and reduced cone cell death. In contrast, overexpression of SOD2 or Catalase alone in the mitochondria of photoreceptors did not significantly reduce oxidative damage or cone cell death.

Various SODs have been overexpressed in other tissues in an attempt to reduce oxidative damage. Overexpression of SOD1 provides protection against oxidative stress in some situations,^{17–20} but increases the vulnerability of some tissues to other types of oxidative stress.^{21,22} Tissues with low levels of glutathione peroxidase might be expected to be intolerant to overexpression of SOD1, because an imbalance between SOD1 and glutathione peroxidase can increase levels of H₂O₂.²³ This may be part of the explanation for the deleterious effects of overexpression SOD1 in models of RP, but it appears that the nature and severity of the oxidative stress is also important, because overexpression of SOD1 reduced oxidative damage from severe oxidative stress.¹⁶ In primary hippocampal neuron cultures, overexpression of SOD1 reduced cyanide toxicity, but increased toxicity from kainic acid or oxygen/glucose deprivation.²⁴ Interestingly, the combination of increased expression of SOD1 and cyanide induced increased levels of glutathione peroxidase, whereas increased SOD1 and kainic acid did not. Therefore, it appears that the tissue, the type of oxidative stress, and its severity may all influence the impact of overexpression of SOD1.

In mice with experimental allergic encephalomyelitis and optic neuritis and also mice in which the NADH-ubiquinone oxidoreductase complex I of the respiratory chain has been knocked down in retinal ganglion cells, overexpression of SOD2 in ganglion cells reduced ganglion cell death and optic nerve degeneration.^{25,26}

This differs from the situation in cones subjected to hyperoxia after death of rods in which we found that overexpression of SOD2 alone increased oxidative damage and failed to improve cone function or survival.

Mice deficient in SOD3 but not those deficient in SOD1, show increased susceptibility to lung damage from hyperoxia²⁷ and brain damage from ischemia/reperfusion.²⁸ Overexpression of SOD3 protects lungs from several types of injury, and it has been postulated that many insults lead to high levels of reactive oxygen species in the interstitial space of lungs, which could best be neutralized by SOD3, which is secreted.^{29–31} Similarly, high levels of reactive oxygen species have been demonstrated in the extracellular space in association with ischemia–reperfusion, and overexpression of SOD3 has provided benefit.³² However, deficiency of SOD3 does not increase susceptibility of the retina to paraquat or hyperoxia (A. Dong and P.A. Campochiaro, unpublished results), whereas deficiency of SOD1 markedly increases retinal susceptibility to those sources of oxidative stress,¹⁶ causing us to eliminate *Sod3* as a possible transgene for our application. However, *Sod3* gene transfer may have some potential usefulness for chronic inflammatory conditions affecting the inner retina; while overexpression of SOD3 alone had no significant effect on ganglion cell or axon loss in mice with chronic experimental allergic encephalomyelitis, when combined with overexpression of Catalase, the effects were greater than the effects of overexpression of Catalase alone.³³

Thus, it appears that the effects of overexpressing SODs can vary considerably depending upon the situation. Our data indicate that overexpression of SOD1 or 2 alone in photoreceptors can exacerbate oxidative damage in cones after rods have degenerated and accelerate retinal degeneration. However, coexpression of SOD2 and Catalase in the mitochondria of photoreceptors strongly promotes cone survival and maintenance of cone function in a model of RP. This suggests that antioxidant gene therapy is a good therapeutic approach for RP, but must be designed and tested carefully before testing in clinical trials.

MATERIALS AND METHODS

Generation of transgenic mice. Mice were treated in accordance with the Association for Research in Vision and Ophthalmology Statement for the Use of Animals in Research and the US National Institutes of Health Guide for the Care and Use of Laboratory Animals. Mice carrying a β -actin promoter/human *Sod1* transgene [C57BL/6-TgN(SOD1)3Cje/J mice, *Sod1*(+/-) mice] were purchased from Jackson Laboratories (Bar Harbor, ME) and crossed with *rd1*^{+/+} mice in a C57BL/6 background to obtain *Sod1*(+/-)-*rd1*^{+/+} mice.

Full-length murine *Sod2* cDNA was generated by reverse transcription–PCR of mouse retinal RNA, cloned into Topo TA cloning vector (Invitrogen, Carlsbad, CA), and sequenced. The *Bam*HI and *Hind*III fragment was released from Topo TA vector and ligated into *pTRE2* vector (Clontech, Mountain View, CA) containing the *TRE*. After sequencing, a fragment containing *TRE*, *Sod2*, and a 1.2 kb β -globin poly A signal was released from *pTRE2* to provide the *TRE/Sod2* construct that was used to generate transgenic mice in the Johns Hopkins University Transgenic Mouse Core Facility.

The *MCAT* plasmid, also known as *poCAT*, which contains human *Catalase* gene with the *ornithine transcarbamylase leader sequence* at its 5' end and without the *peroxisomal localization signal* at its 3' end to provide targeting to mitochondria; transgenic mice with ubiquitous expression

Catalase in mitochondria have a long lifespan.³⁴ The *MCAT* construct was ligated into *pTRE2*. After sequencing, a fragment containing *TRE*, *MCAT*, and a 1.2 kb β -globin poly A signal was released from *pTRE2* to provide the *TRE/Catalase* construct that was used to generate transgenic mice in the Johns Hopkins University Transgenic Mouse Core Facility.

Founder mice were mated with C57BL/6 mice to generate founder lines. Mice from each line were crossed with mice from the *IRBP/rtTA* driver line to generate *IRBP/rtTA-TRE/Sod2* and *IRBP/rtTA-TRE/Catalase* double transgenic mice. Mice from double transgenic lines were given 2 mg/ml in their drinking water and real-time PCR was done to identify *IRBP/rtTA-TRE/Sod2* and *IRBP/rtTA-TRE/Catalase* lines with strong, inducible transgene expression.

Genotyping of mice. Genotyping was done by PCR of tail DNA using the following primers: *human Sod1* (forward:5'-CATCAGCCC TAATCCATCTGA-3', reverse:5'-CGCGACTAACAAATCAAAGTGA-3'); *TRE/Sod2* (forward:5'-CACGCTGTTTGGACCTCC-3', reverse:5'-GCTT GATAGCCTCCAGCAAC-3'); *TRE/Catalase* (forward:5'-TCTGGAGAA GTGCGGAGATT-3', reverse:5'-AGTCAGGGTGGACCTCAGTG-3'), and *IRBP/rtTA* (forward:5'-GTTTACCGATGCCCTTGAATTGACGA GT-3', reverse:5'-GATGTGGCGAGATGCTCTTGAAGTCTGGTA-3'). To distinguish homozygous *rd1*, and wild-type mice, the PCR fragment generated with forward, 5'-CATCCACCT GAGCTCACAGAAAG-3' and reverse, 5'-GCCTACAACAGAGGAGCTT CTAGC-3' was digested with *Dde*I or *Bsa*AI. To distinguish homozygous *rd10*, heterozygous *rd10*, and wild-type mice, the PCR fragment generated with forward, 5'-CTTTCTATTCTCTGTCAGCAAAGC-3' and reverse, 5'-CATGAGTAGGGTAAACATGGTCTG-3' was digested with *Cfo*I.

Mutant *rd10* mice with inducible expression of SOD2, Catalase, or both. *Rd10*^{+/+} mice (Jackson Laboratories, Bar Harbor, ME) were used in an elaborate mating scheme to generate *TRE/Sod2*(+/-)-*TRE/Catalase*(+/-) *rd10*^{+/+} mice and *IRBP/rtTA*(+/-)-*rd10*^{+/+} mice. These mice were crossed to generate *-rd*^{+/+} mice that did not carry either the *TRE/Sod2* or *TRE/Catalase* transgenes, but that which carried only the *TRE/Sod2* transgene, or only the *TRE/Catalase* transgene, or that which carried both the *TRE/Sod2* and *TRE/Catalase* transgenes. Starting at P10, mothers of these mice were given 2 mg/ml of doxycycline in their drinking water. At P21, the mice were separated from their mothers and given drinking water containing 2 mg/ml of doxycycline. Transgene product was measured by immunoblots of retinal homogenates at P25.

Immunoblots. For *Sod1*(+/-)-*rd1*^{+/+} mice, whole retinas were dissected and placed in 50 μ l of lysis buffer (10 mmol/l Tris, pH 7.2, 0.5% Triton X-100, 50 mmol/l NaCl, and 1 mmol/l EDTA) containing a proteinase inhibitor mixture tablet (Roche, Indianapolis, IN). After three freeze/thaw cycles and homogenization, samples were microfuged at 14,000g for 5 minutes at 4°C and the protein concentration of the supernatant was measured using a Bio-Rad Protein Assay Kit (Bio-Rad, Hercules, CA). For all of the other mice, a Mitochondrial Isolation Kit for Tissue (Pierce, Rockford, IL) was used according to the manufacturer's instructions to isolate retinal mitochondria. For each sample, 20 μ g of protein was resolved by sodium dodecyl sulfate–polyacrylamide gel electrophoresis and transferred to a nitrocellulose membrane (Hybond-ECL; Amersham Biosciences, Piscataway, NJ). Rabbit polyclonal antihuman SOD1 (1:1,000; Chemicon International, Temecula, CA), rabbit polyclonal anti-SOD2 (1:10,000; Abcam, Cambridge, MA), or rabbit polyclonal antihuman Catalase (1:2,000; Athens Research Technology, Athens, GA) were used as primary antibody. The secondary antibody was a horseradish peroxidase–coupled goat anti-rabbit IgG (1:1,000; Cell Signaling, Danvers, MA). Blots were incubated in SuperSignal Western Pico Lumino/Enhancer solution (Pierce, Rockford, IL) and exposed to X-ray film (Eastman-Kodak, Rochester, NY). To assess loading levels of protein, SOD1 blots were stripped and incubated with

polyclonal rabbit anti- β -actin antibody (1:5,000; Cell Signaling, Danvers, MA) followed by horseradish peroxidase-coupled goat antirabbit IgG and other blots were stripped and incubated with mouse monoclonal anti-COX4 (1:5,000; Abcam, Cambridge, MA) followed by horseradish peroxidase-coupled antimouse IgG (1:2,000; Cell Signaling, Danvers, MA).

Assessment of superoxide radicals with hydroethidine. As previously described,^{12,35} *in situ* production of superoxide radicals was evaluated using hydroethidine, which in the presence of superoxide radicals is converted to ethidium, which binds DNA and emits red fluorescence at ~600 nm. Briefly, mice were given two 20-mg/kg intraperitoneal injections 30 minutes apart of freshly prepared hydroethidine (Invitrogen, Carlsbad, CA) and euthanized 18 hours after injection. Eyes were rapidly removed and 10- μ m frozen sections were fixed in 4% paraformaldehyde for 20 minutes at room temperature, rinsed with phosphate-buffered saline (PBS), and counterstained for 5 minutes at room temperature with the nuclear dye Hoechst 33258 (1:10,000; Sigma, St Louis, MO). After rinsing in PBS, slides were mounted with Aquamount solution and evaluated for fluorescence (excitation: 543 nm, emission >590 nm) with a LSM 510 META confocal microscope. Images were captured using the same exposure time for each section.

ELISA for protein carbonyl content. Retinas were homogenized in lysis buffer and centrifuged at 16,000g for 5 minutes at 4°C and the protein concentration of the supernatant was measured using a Bio-Rad Protein Assay Kit (Bio-Rad). Samples were adjusted to 4mg/ml by dilution with Tris-buffered saline, and protein carbonyl content was determined by ELISA, as previously described.^{4,10}

Measurement of cone cell density. Cone density was measured as previously described.⁴ Briefly, each mouse was euthanized, and eyes were carefully removed and were fixed in 4% paraformaldehyde for 3 hours or overnight at 4°C. After washing with PBS, the cornea, iris, and lens were removed. A small triangle cut was made at 12:00 in the retina for future orientation and after four cuts equidistant around the circumference, the entire retina was carefully dissected from the eye cup and any adherent retinal pigmented epithelium was removed. Retinas were placed in 10% normal goat serum in PBS for 30 minutes at room temperature, incubated for 1 hour at room temperature in 1:100 rhodamine-conjugated peanut agglutinin (Vector Laboratories, Burlingame, CA) in PBS containing 1% normal goat serum, and flat mounted. The retinas were examined with a Zeiss LSM 510 META confocal microscope (Carl Zeiss, Oberkochen, Germany) with a Zeiss Plan-Apochromat 20 \times /0.75 NA objective using an excitation wavelength of 543 nm to detect rhodamine fluorescence. Images were acquired in the frame scan mode. The number of cones was determined by image analysis within four 230 mm \times 230 mm squares located 1 mm (*rd1* mice) or 0.5 mm (wild-type and *rd10* mice) superior, inferior, temporal, and nasal to the center of the optic nerve. The investigator was masked with respect to experimental group.

Measurement of ONL thickness. ONL thickness was measured, as previously described.⁵ Mice were euthanized, a mark was placed at 12:00 at the corneal limbus, and eyes were removed and embedded in optimal cutting temperature compound. Ten-micrometer frozen sections were cut perpendicular to the 12:00 meridian through the optic nerve and fixed in 4% paraformaldehyde. The sections were stained with hematoxylin and eosin, examined with an Axioskop microscope (Zeiss, Thornwood, NY), and images were digitalized using a three-charge-coupled device color video camera (IK-TU40A; Toshiba, Tokyo, Japan) and a frame grabber. Image-Pro Plus software (Media Cybernetics, Silver Spring, MD) was used to outline the ONL. ONL thickness was measured at six locations, 25% (S1), 50% (S2), and 75% (S3) of the distance between the superior pole and the optic nerve and 25% (I1), 50% (I2), and 75% (I3) of the distance between the inferior pole and the optic nerve.

Recording of ERGs. An Espion ERG Diagnosys machine (DiagnoSYS LLL, Littleton, MA) was used to record ERGs as previously described.^{4,5,7,36} For

scotopic recordings, mice were adapted to dark overnight, and for photopic recordings, mice were adapted to background white light at an intensity of 30 cd/m² for 10 minutes. The mice were anesthetized with an intraperitoneal injection of ketamine hydrochloride (100 mg/kg body weight) and xylazine (5 mg/kg body weight). Pupils were dilated with Midrin P containing of 0.5% tropicamide and 0.5% phenylephrine, hydrochloride (Santen Pharmaceutical, Osaka, Japan). The mice were placed on a pad heated to 39°C and platinum loop electrodes were placed on each cornea after application of Gonioscopic prism solution (Alcon Labs, Fort Worth, TX). A reference electrode was placed subcutaneously in the anterior scalp between the eyes and a ground electrode was inserted into the tail. The head of the mouse was held in a standardized position in a ganzfeld bowl illuminator that ensured equal illumination of the eyes. Recordings for both eyes were made simultaneously with electrical impedance balanced. Scotopic ERGs were recorded at six intensity levels of white light ranging from -3.00 to 1.40 log cd-s/m². Six measurements were averaged at each flash intensity. Low background photopic ERGs were recorded at 1.48 log cd-s/m² under a background of 10 cd/m². Sixty photopic measurements were taken and the average value was recorded.

Statistical analysis. Statistical comparisons were done using Tukey-Kramer's test for multiple comparisons and unpaired Student's *t*-test or Welch's *t*-test for two comparisons. Differences test for multiple comparisons were judged statistically, significant at *P* < 0.05 or *P* < 0.01.

ACKNOWLEDGMENTS

This work was supported by grants R01 EY05951 (P.A.C.) and P01 AG01751 (P.S.R.) from the National Institutes of Health and a gift from and William Lake. S.U. is a Bausch and Lomb Japan Vitreoretinal Research Fellow and was supported by The Osaka Medical Research Foundation for Incurable Diseases. P.A.C. is the George S. and Dolores Dore Eccles Professor of Ophthalmology and Neuroscience.

REFERENCES

1. Yu, DY, Cringle, SJ, Su, EN and Yu, PK (2000). Intraretinal oxygen levels before and after photoreceptor loss in the RCS rat. *Invest Ophthalmol Vis Sci* **41**: 3999–4006.
2. Yu, DY, Cringle, SJ, Valter, K, Walsh, N, Lee, D and Stone, J (2004). Photoreceptor death, trophic factor expression, retinal oxygen status, and photoreceptor function in the P23H rat. *Invest Ophthalmol Vis Sci* **45**: 2013–2019.
3. Shen, J, Yan, X, Dong, A, Petters, RM, Peng, YW, Wong, F, et al. (2005). Oxidative damage is a potential cause of cone cell death in retinitis pigmentosa. *J Cell Physiol* **203**: 457–464.
4. Komeima, K, Rogers, BS, Lu, L and Campochiaro, PA (2006). Antioxidants reduce cone cell death in a model of retinitis pigmentosa. *Proc Natl Acad Sci USA* **103**: 11300–11305.
5. Komeima, K, Rogers, BS and Campochiaro, PA (2007). Antioxidants slow photoreceptor cell death in mouse models of retinitis pigmentosa. *J Cell Physiol* **213**: 809–815.
6. Ohno-Matsui, K, Hirose, A, Yamamoto, S, Saikia, J, Okamoto, N, Gehlbach, P, et al. (2002). Inducible expression of vascular endothelial growth factor in photoreceptors of adult mice causes severe proliferative retinopathy and retinal detachment. *Am J Pathol* **160**: 711–719.
7. Okoye, G, Zimmer, J, Sung, Gehlbach, P, Deering, T, Nambu, N, et al. (2003). Increased expression of BDNF preserves retinal function and slows cell death from rhodopsin mutation or oxidative damage. *J Neurosci* **23**: 4164–4172.
8. Oshima, Y, Oshima, S, Nambu, H, Kachi, S, Takahashi, K, Umeda, N, et al. (2005). Different effects of angiopoietin 2 in different vascular beds in the eye; new vessels are most sensitive. *FASEB J* **19**: 963–965.
9. Dong, A, Shen, J, Krause, M, Hackett, SF and Campochiaro, PA (2007). Increased expression of glial cell line-derived neurotrophic factor protects against oxidative damage-induced retinal degeneration. *J Neurochem* **103**: 1041–1052.
10. Lu, L, Oveson, BC, Jo, YJ, Lauer, T, Usui, S, Komeima, K, et al. (2008). Increased expression of glutathione peroxidase 4 strongly protects retina from oxidative damage. *Antioxid Redox Signal* (epub ahead of print).
11. Pietch, A, Dessy, C, Havaux, X, Feron, O and Balligand, JL (2003). Differential regulation of nitric oxide synthases and their allosteric regulators in heart and vessels of hypertensive rats. *Cardiovasc Res* **57**: 456–467.
12. Komeima, K, Usui, S, Shen, J, Rogers, BS and Campochiaro, PA (2008). Blockade of neuronal nitric oxide synthase reduces cone cell death in a model of retinitis pigmentosa. *Free Radic Biol Med* **45**: 905–912.
13. Levine, RL (2002). Carbonyl modified proteins in cellular regulation, aging, and disease. *Free Radic Biol Med* **32**: 790–796.
14. Buss, H, Chan, TP, Sluis, KB, Domigan, NM and Winterbourn, CC (1997). Protein carbonyl measurement by a sensitive ELISA method. *Free Radical Biol Med* **23**: 361–366.
15. Lu, L, Hackett, SF, Mincey, A, Lai, H and Campochiaro, PA (2006). Effects of different types of oxidative stress in RPE cells. *J Cell Physiol* **206**: 119–125.

16. Dong, A, Shen, J, Krause, M, Akiyama, H, Hackett, SF, Lai, H, *et al.* (2006). Superoxide dismutase 1 protects retinal cells from oxidative damage. *J Cell Physiol* **208**: 516–526.
17. Przedborski, S, Kostic, V, Jackson, LV, Naini, AB, Simonetti, S, Fahn, S, *et al.* (1992). Transgenic mice with increased Cu/Zn-superoxide dismutase activity are resistant to N-methyl-4-phenyl-1,2,3,6-tetrahydropyridine-induced neurotoxicity. *J Neurosci* **12**: 1658–1667.
18. Cadet, JL, Sheng, P, Ali, S, Rothman, R, Carlson, E and Epstein, CJ (1994). Attenuation of methamphetamine-induced neurotoxicity in copper/zinc superoxide dismutase transgenic mice. *J Neurochem* **62**: 380–383.
19. Schwartz, PJ, Reaume, A, Scott, R and Coyle, JT (1998). Effects of over- and under-expression of Cu,Zn-superoxide dismutase on the toxicity of glutamate analogs in transgenic mouse striatum. *Brain Res* **789**: 32–39.
20. Venugopal, SK, Wu, J, Catana, AM, Eisenbud, L, He, SQ, Duan, YY, *et al.* (2007). Lentivirus-mediated superoxide dismutase1 gene delivery protects against oxidative stress-induced liver injury in mice. *Liver Int* **27**: 1311–1322.
21. Elroy-Stein, O and Groner, Y (1988). Impaired uptake in PC12 cells overexpressing human Cu/Zn-superoxide dismutase—implication for gene dosage effect in Down syndrome. *Cell* **52**: 259–267.
22. Rader, RK and Lanthorn, TH (1989). Experimental ischemia induces a persistent depolarization blocked by decreased calcium and NMDA antagonists. *Neurosci Lett* **99**: 125–130.
23. de Haan, JB, Cristiano, F, Iannello, R, Bladier, C, Kelner, MJ and Kola, I (1996). Elevation in the ratio of Cu/Zn-superoxide dismutase to glutathione peroxidase activity induces features of cellular senescence and this effect is mediated by hydrogen peroxide. *Hum Mol Genet* **5**: 283–292.
24. Zemlyak, I, Nimon, V, Brooke, S, Moore, T, McLaughlin, J and Sapolsky, R (2006). Gene therapy in the nervous system with superoxide dismutase. *Brain Res* **1088**: 12–18.
25. Qi, X, Lewin, AS, Sun, L, Hauswirth, WW and Guy, J (2004). SOD2 gene transfer protects against optic neuropathy induced by deficiency of complex I. *Ann Neurol* **56**: 182–191.
26. Qi, X, Lewin, AS, Sun, L, Hauswirth, WW and Guy, J (2007). Suppression of mitochondrial oxidative stress provides long-term neuroprotection in experimental optic neuritis. *Invest Ophthalmol Vis Sci* **48**: 681–691.
27. Carlsson, LM, Jonsson, J, Edlund, T and Marklund, SL (1995). Mice lacking extracellular superoxide dismutase are more susceptible to hyperoxia. *Proc Natl Acad Sci USA* **92**: 6264–6268.
28. Sheng, H, Brady, TC, Pearlstein, RD, Crapo, JD and Warner, DS (1999). Extracellular superoxide dismutase deficiency worsens outcome from focal cerebral ischemia in the mouse. *Neurosci Lett* **267**: 13–16.
29. Bowler, RP, Nicks, M, Warnick, K and Crapo, JD (2002). Role of extracellular superoxide dismutase in bleomycin-induced pulmonary fibrosis. *Am J Physiol Lung Cell Mol Physiol* **282**: L719–L726.
30. Rabbani, ZN, Anscher, MS, Folz, RJ, Archer, E, Huang, H, Chen, L, *et al.* (2005). Overexpression of extracellular superoxide dismutase reduces acute radiation induced lung toxicity. *BMC Cancer* **5**: 59.
31. Auten, RL, O'Reilly, MA, Oury, TD, Nozik-Grayck, E and Whorton, MH (2006). Transgenic extracellular superoxide dismutase protects postnatal alveolar epithelial proliferation and development during hyperoxia. *Am J Physiol Lung Cell Mol Physiol* **290**: L32–L40.
32. Agrawal, RS, Muangman, S, Layne, MD, Melo, L, Perrella, MA, Lee, RT, *et al.* (2004). Pre-emptive gene therapy using recombinant adeno-associated virus delivery of extracellular superoxide dismutase protects heart against ischemia reperfusion injury, improves ventricular function and prolongs survival. *Gene Ther* **11**: 962–969.
33. Qi, X, Sun, L, Lewin, AS, Hauswirth, WW and Guy, J (2007). Long-term suppression of neurodegeneration in chronic experimental optic neuritis: antioxidant gene therapy. *Invest Ophthalmol Vis Sci* **48**: 5360–5370.
34. Schriener, SE, Linford, NJ, Martin, GM, Treuting, P, Ogburn, CE, Emond, M, *et al.* (2005). Extension of murine life span by overexpression of catalase targeted to mitochondria. *Science* **308**: 1909–1911.
35. Behrens, MM, Ali, SS, Dao, DN, Lucero, J, Shekhtman, G, Quick, KL, *et al.* (2008). Ketamine-induced loss of phenotype of fast-spiking interneurons is mediated by NADPH-oxidase. *Science* **318**: 1645–1647.
36. Ueno, S, Pease, ME, Wersinger, DM, Masuda, T, Viores, SA, Licht, T, *et al.* (2008). Prolonged blockade of VEGF family members does not cause identifiable damage to retinal neurons or vessels. *J Cell Physiol* **217**: 13–22.